J. Fluid Mech. (1971), vol. 50, part 3, pp. 579–608
Printed in Great Britain

Spin-up of a stratified fluid: theory and experiment

By GEORGE BUZYNA
Geophysical Fluid Dynamics Institute, Florida State University, Tallahassee, Florida

AND GEORGE VERONIS
Department of Geology and Geophysics, Yale University, New Haven, Conn.

(Received 5 October 1970 and in revised form 1 June 1971)

Stratified spin-up, the process of adjustment of a uniformly rotating stratified fluid to an abrupt change in the rotation of the container, is important in many geophysical contexts. An experimental study of this process is presented here for the case where a linearly stratified salt solution is enclosed in a cylindrical container whose rotation rate is changed by a small amount. Results are presented for a limited range of values of B, the internal Froude number, which measures the ratio of the frequencies due to buoyancy and rotation. The experimental study is augmented by a theoretical treatment of idealized models which clarify the more fundamental physical processes that occur. The response of a stratified fluid is faster than that of a homogeneous fluid but the adjustment is limited to layers near the bottom and top boundaries the thickness of which is determined by the value of B. A comparison of the experimental results with the theories of Holton, Walin and Sakurai is also made and it is shown that for the present physical arrangement (insulated side walls) the theories of the latter two authors agree much more closely with experiment than does the theory of Holton. However, all three theories tend to over-estimate the azimuthal displacement in the regions near the upper and lower boundaries where the spin-up is most rapid. The Sweet–Eddington circulation, which accompanies the ideal state of rigid-body rotation, can be significant under normal laboratory conditions and it was necessary to correct some of the spin-up results for this effect. The circulation in the vertical plane is described qualitatively.

1. Introduction, summary and conclusions

The process of adjustment of a rotating fluid to an imposed change in the rotation rate is important for understanding transient geophysical flows. A simple model for the study of the flow associated with such a change has been presented by Greenspan & Howard (1963). In their study the uniform rotation rate of a right cylindrical container of homogeneous fluid was increased abruptly to a slightly different value. They analyzed the response of the fluid to this change and called the adjustment process the spin-up of the fluid. The present paper reports an experimental study of the spin-up of a stratified fluid and an explanation of the flow in terms of simple analytic models.

Although Greenspan & Howard presented the first thorough analysis of the adjustment process, experiments in which the rotation of the container was abruptly changed from zero to some finite value had been performed many years earlier by Ekman (1906). By comparing the responses of homogeneous and stably stratified fluids he hoped to measure the effect of stratification on the diffusion of momentum from the boundary regions into the interior of the fluid.

Ekman suspended a light aluminium vane at the mid-level of the fluid in each case and measured the rate at which vorticity was transferred from the Ekman layer (as we now call it) to the level at which the vane was located. He concluded that stratification served to inhibit the penetration of boundary effects. To support his experimental findings he included an analysis of diffusion of momentum from the bottom boundary upward and described the difference between the results for the homogeneous and stratified cases in terms of different effective diffusion coefficients. He was evidently unaware of the secondary circulation which we now term the spin-up process.

Some years later Pettersson (1931)† repeated Ekman's experiments and made more careful and detailed observations of the induced flow in the interior regions of the fluid. He concluded that Ekman's findings were correct, i.e. the stratification inhibited the upward transfer of momentum. However, he also observed the secondary spin-up circulation and realized that the upward transfer of momentum was due to this circulation rather than to the vertical diffusion of momentum. Although Pettersson sketched a somewhat inaccurate picture of the secondary circulation (the fluid was thrown outward near the bottom boundary, flowed upward near the side wall, turned horizontally inward and eventually was sucked down into the bottom boundary layer via a narrow column near the centre), he had a pretty clear picture of the manner in which the rotation was transmitted to the main body of the fluid. A quotation from his paper follows: "From the experiments here described we may infer, that turbulence probably has very little to do with the great increase in μ experienced, when the water in the rotating cylinder is changed from a stratified to a homogeneous condition. Instead of a transmission of momentum upwards by friction, as at a strictly laminar motion, we have, in the latter case, a transport of momentum, not by small vortices but by a vertical circulation passing through the whole of the rotating water-column. The effect is somewhat analogous to what happens at an experiment, in which the heat-conductivity of a liquid is to be determined, but where convection currents are not completely excluded.

"This result is much to be regretted, since it seems to close an apparently very promising and simple way for studying in the laboratory, how turbulence is generated and how it is influenced by the vicinity to boundaries, absolute as well as relative, if by the latter expression to transition-layers between strata of different densities may be denoted."

Although Pettersson did not analyze his results quantitatively, he pointed out the correct qualitative nature of the process and he presented additional experimental observations of such features as the instability which occurs after the initiation of spin-up in a two-layer fluid.

† The existence of this paper was pointed out to us by Pierre Welander.

The spin-up of a stratified fluid differs from the corresponding process for a homogeneous fluid in some important respects. In the first place, the word 'spin-up' itself acquires a different meaning. When the fluid is homogeneous, the bulk of the fluid responds to a small change, $\Delta\Omega$, in the rotation rate in a time of order $E^{-\frac{1}{2}}\,\Omega^{-1}$, where E is the Ekman number (defined in §2) and $\Omega - \Delta\Omega$ and Ω are the initial and final rotation rates of the fluid. Residual wave motions are eliminated after an interval which may be as long as that corresponding to the diffusion time ($E^{-1}\,\Omega^{-1}$) for the fluid. If the latter are ignored, the spin-up time may be defined as the time required for the bulk of the fluid to rotate with angular velocity $\Omega - e^{-1}\Delta\Omega$.

For a stratified fluid the process is considerably more complicated. At the initial instant all of the fluid rotates with the angular velocity $\Omega - \Delta\Omega$. After a time interval of order $E^{-\frac{1}{2}}\,\Omega^{-1}$, the angular velocity of the fluid at each point levels off to a value given by $\Omega - \alpha\Delta\Omega$, where $\alpha(\leqslant 1)$ is a function of radius and height. The spin-up time is defined here as the time required for a particle of fluid to rotate with angular velocity $\Omega - e^{-1}\alpha\Delta\Omega$.

Diffusion effects will ultimately cause all the fluid to rotate with angular velocity Ω; i.e. significant changes in the angular velocity of the fluid particles will take place between the spin-up time and the diffusion time.

Some investigators have interpreted spin-up time as the time required for all the fluid to achieve rigid-body rotation with angular velocity Ω and for all of the residual wave motions to be dissipated. In this case the spin-up time is the diffusion time even for homogeneous fluids. Others have defined the spin-up time as the time required for all of the fluid to rotate with angular velocity $\Omega - e^{-1}\Delta\Omega$. Here, the spin-up time for a homogeneous fluid is as we have defined it above but for a stratified fluid some regions will not have been spun up before a diffusion time has elapsed. Still others have accepted the definitions that we have given above. For this situation the spin-up time for a stratified fluid can differ from point to point. Furthermore, as we shall see shortly, the spin-up time for a stratified fluid is shorter than that for a homogeneous fluid if the presently adopted definition is used. In any event, no confusion need arise as long as the particular interpretation of spin-up time is clearly given.

In the following section the Navier–Stokes equations for a stratified fluid where the Boussinesq approximation is applicable are made dimensionless and the appropriate non-dimensional parameters are introduced. The model for stratified spin-up as derived by Walin (1969) and Sakurai (1969) is then stated and their solution is given. It is possible to obtain the qualitative character of the spin-up of the fluid by treating the idealized model of a horizontally infinite layer of fluid when spatially harmonic forcing is applied at the top and bottom boundaries uniformly in time for $t > 0$. It is easily shown in this case that penetration of boundary effects into the interior of the fluid is restricted to a layer of fluid whose thickness is determined by the stratification (the parameter B) and by the scale (or the wave-number k) of the forcing at the boundary. When $Bk \gg 1$, only a limited penetration occurs and the spin-up time as defined above is considerably shorter than it is for a homogeneous fluid. When $Bk \ll 1$, the response is similar to that for a homogeneous fluid. A simple physical argument for the spin-up process is presented and the reason for the decreased spin-up time in the stratified case is easily understood in terms of this model.

A second horizontally infinite model, with the boundary forcing independent of one of the horizontal directions, is constructed to simulate the experimental situation. Here, boundary forcing is given as a zonal velocity uniform in the y direction but cyclic in the x direction (shown as the curve marked $t = 0$ in figure 2 (a)). The sharp decrease in the zonal velocity profile near $x = 1$ is meant to simulate the effect of the diffusive processes near the side wall shortly after the initial instant in the experiment. The structure of the interior flow is shown to be consistent with the conclusions drawn from the situation with harmonic forcing. In particular, when $B = O(1)$ smaller-scale motions ($k \gg 1$) penetrate less deeply into the fluid and they decay in a time much shorter than do the larger-scale motions. Consequently, as the spin-up process develops, the initially asymmetric response becomes smoothed and the interior flow has no sharp gradients. When $B \ll 1$ the response approaches that of a homogeneous fluid.

After the description of the experimental apparatus and procedure in §4, an overall view of the experiments is presented in §5. First, we outline our observations of the relative Sweet–Eddington flow, i.e. the flow caused by diffusion in a fluid which is otherwise in a state of rigid-body rotation. With $\Omega \geqslant 2$ rad sec^{-1} in our experiments the magnitude of the Sweet–Eddington flow is large enough to affect the spin-up circulation. Hence, experiments with larger rotation rates were abandoned. Second, we describe the data used for obtaining the spin-up times at different points in the fluid. A discussion of the azimuthal displacement *vs.* radius is followed by our qualitative observations of the circulation pattern. The foregoing points are discussed in terms of the simple models introduced in §3.

In §6 a comparison between theory and experiment is given. Observations of displacement *vs.* time at mid-level and mid-radius agree very well with Walin's results and not so well with Holton's. Similar observations made at a level just outside the Ekman layer show a disparity between both theories and the experiments. The latter typically yield a smaller displacement than the theories do.

Since the spin-up time is an integral measure of the response of the fluid, it provides a grosser comparison between theory and experiment than does the time-displacement data. Over the range of B explored here ($0{\cdot}4 \leqslant B \leqslant 1{\cdot}4$) Walin's calculated spin-up times are in better agreement with experimentally determined times at levels near the Ekman layer than at mid-level. Holton's spin-up times are everywhere too large.

Curves of azimuthal displacement *vs.* radius show that the best agreement between theory and experiment is obtained at mid-radius. Adding the correction due to side-wall diffusion to the theoretical results near the outer boundary improves the comparison there significantly. However, the theory generally overestimates the azimuthal displacement.

From the foregoing we can conclude that the linear theoretical analyses which have been presented by Walin and Sakurai are in reasonably good agreement with experiments but yield small quantitative discrepancies. The disparity is greatest just outside the Ekman boundary layers and near the centre and the side wall of the tank. Hence we must conclude that the theories describe the larger-scale response better than they do the smaller-scale response because the latter determines the behaviour in the regions of largest discrepancy. Since non-linear processes in the corner, where the flow turns into the interior from the Ekman layer, are small-scale phenomena, it appears likely that the discrepancy can be attributed to them.

We can also conclude from this study that the solution presented by Walin and Sakurai is generally in better agreement with experiment than is Holton's solution. As Sakurai has shown, Holton's solution is not appropriate for the case where the side-wall boundary is non-conducting. Since the latter boundary condition applies to our experiments, it is perhaps not appropriate to compare the results with Holton's solution. However, Holton's experiments also involved non-conducting boundaries and he claimed considerably better agreement between his theory and experiments than we were able to find between his theory and our experiments.

The paper concludes with a section on the experimental difficulties which we encountered. The response of the turn-table to a change in the rotation rate, errors associated with the position of the dye, drag due to the wires, and other problems are present in the homogeneous spin-up experiments as well as in the stratified ones. Hence, spin-up experiments with a homogeneous fluid are described and form a basis for comparison and determination of some of the experimental errors. Some of the problems specifically associated with the density gradients in the fluid round out the discussion.

2. Equations of motion and the spin-up solution

We start with the Navier–Stokes equations for a Boussinesq fluid in a rotating system and incorporate the centrifugal force terms into the pressure gradient. For solid-body rotation we assume that surfaces of constant density are essentially parallel to the horizontal. With the Boussinesq approximation the conservation equation for the concentrations of the stabilizing solute can be written in terms of an effective density. Then the equations which determine the flow are

$$\frac{\partial \mathbf{v}}{\partial t}+\mathbf{v}\,.\,\nabla\mathbf{v}+2\mathbf{\Omega}\times\mathbf{v} = -\frac{1}{\rho_r}\nabla p - g\frac{\hat{\rho}}{\rho_r}\,\mathbf{i}_z+\nu\nabla^2\mathbf{v}, \tag{2.1}$$

$$\nabla\,.\,\mathbf{v} = 0, \tag{2.2}$$

$$\frac{\partial \hat{\rho}}{\partial t}+\mathbf{v}\,.\,\nabla\hat{\rho}+w\frac{\partial\bar{\rho}}{\partial z} = \kappa\nabla^2\hat{\rho}, \tag{2.3}$$

where ρ_r is a (constant) reference density and $\hat{\rho}$ is the density perturbation which occurs as a result of the motion. The basic rotation, $\mathbf{\Omega}$, and gravity are directed along the z axis with unit vector $\mathbf{i}_z$. The term $\partial\bar{\rho}/\partial z$ in (2.3) is the constant stabilizing gradient and will be written as

$$\frac{1}{\rho_r}\frac{\partial\bar{\rho}}{\partial z} = -\frac{4}{\rho_r}\frac{\Delta\rho}{L}, \tag{2.4}$$

where $8\Delta\rho$ is the amplitude of the density difference from bottom to top and $2L$ is the height of the container.

The equations are conveniently non-dimensionalized by the definitions

$$\frac{\partial}{\partial t} = \Omega \frac{\partial}{\partial t'}, \quad \mathbf{v} = V\mathbf{v}', \quad p = \rho_r L\Omega V p', \quad \hat{\rho} = \frac{2\Delta\rho}{\rho_r} B\rho', \quad \nabla = \frac{1}{L}\nabla', \tag{2.5}$$

where the primes denote non-dimensional quantities. If the scales for velocity and density fluctuation are related by

$$g\frac{\Delta\rho}{\rho_r}\Big/\Omega V = 1, \tag{2.6}$$

(2.1) and (2.3) take the form (dropping the primes)†

$$\partial\mathbf{v}/\partial t + \epsilon\mathbf{v}.\nabla\mathbf{v} + 2\mathbf{i}_z \times \mathbf{v} = -\nabla p - 2\rho B\mathbf{i}_z + E\nabla^2\mathbf{v}, \tag{2.7}$$

$$\partial\rho/\partial t + \epsilon\mathbf{v}.\nabla\rho - 2Bw = (E/\sigma)\nabla^2\rho, \tag{2.8}$$

where the parameters are defined by

$$\left.\begin{array}{ll} \text{Rossby number} & \epsilon = V/\Omega L, \\ \text{Ekman number} & E = \nu/\Omega L^2, \\ \text{Prandtl number} & \sigma = \nu/\kappa, \end{array}\right\} \tag{2.9}$$

ratio of Brunt–Väisälä to rotational frequencies

$$B = \left(\frac{g\Delta\rho}{\rho_r L\Omega^2}\right)^{\frac{1}{2}} \equiv \left(\frac{-g}{\rho_r}\frac{\partial\bar{\rho}}{\partial z}\right)^{\frac{1}{2}}\Big/2\Omega.$$

The situation of interest is that in which the effect of rotation is dominant and the relative motions are small so that

$$E \ll 1, \quad \epsilon \to 0. \tag{2.10}$$

For a homogeneous fluid (Greenspan & Howard 1963) the spin-up time can be shown to be $O(E^{\frac{1}{2}})$ and a formal substitution of

$$\partial/\partial t' = E^{\frac{1}{2}}\,\partial/\partial t \tag{2.11}$$

simplifies the analysis for deducing the spin-up time. Information in a time scale of $O(\Omega^{-1})$ is lost by the substitution (2.11) but this information has principally to do with inertial oscillations which are not important for the determination of the spin-up time. We make the same substitution in the stratified problem so that (2.7) and (2.8) become

$$E^{\frac{1}{2}}\,\partial\mathbf{v}/\partial t + 2\mathbf{i}_z \times \mathbf{v} = -\nabla p - 2B\rho\mathbf{i}_z + E\nabla^2\mathbf{v}, \tag{2.12}$$

$$E^{\frac{1}{2}}\,\partial\rho/\partial t - 2Bw = (E/\sigma)\nabla^2\rho, \tag{2.13}$$

where ϵ has been set equal to zero.

From this point on, the analysis for spin-up in a right circular container with insulated boundaries can be developed along the lines given by Walin (1969) and Sakurai (1969). The variables are divided into interior and boundary-layer

† The number 2 appears as a coefficient of the Coriolis, gravity and stability terms to preserve a certain symmetry and also for analytical convenience.

contributions, each set is expanded in powers of $E^{\frac{1}{2}}$ and use is made of Ekman boundary-layer theory. The lowest-order interior problem, consistent with the scaling and the boundary conditions, is expressed in terms of the zero-order interior pressure field

$$\nabla_H^2 \dot{p}_0 + \frac{1}{B^2}\,\partial^2 \dot{p}_0/\partial z^2 = 0, \tag{2.14}$$

$$\frac{1}{B^2}\frac{\partial \dot{p}_0}{\partial z} = \pm\, 2\mathbf{i}_z.\nabla\times\mathbf{v} \mp \nabla_H^2 p_0 \quad \text{at} \quad z = \pm\, 1, \tag{2.15}$$

$$\partial \dot{p}_0/\partial r = 0 \quad \text{at} \quad r = a, \tag{2.16}$$

where $\dot{p}_0 \equiv \partial p_0/\partial t$ and the velocity $\mathbf{v}$ in (2.15) is the total velocity which is known at $z = \mp 1$.

To satisfy the non-slip boundary condition at the sides a Stewartson $E^{\frac{1}{4}}$ boundary layer is appended near $r = a$. The equation for this layer (Pedlosky 1967) is

$$\partial v_0^{(\frac{1}{4})}/\partial t = \partial^2 v_0^{(\frac{1}{4})}/\partial \xi^2 \quad \text{near} \quad r = a, \tag{2.17}$$

where $\xi = (a-r)E^{-\frac{1}{4}}$ and $v^{(\frac{1}{4})}$ is the contribution to v_0 of the $E^{\frac{1}{4}}$ layer.

The solution to this problem, as derived by Walin and Sakurai, is

$$v_0 = -r + 2a\sum_{n=1}^{\infty} \frac{\cosh Bm_n z}{\lambda_n J_0(\lambda_n)\cosh Bm_n} J_1(m_n r)\,(e^{-t/\tau_n}-1) + a\,\mathrm{erfc}\left(\frac{\xi}{2t^{\frac{1}{2}}}\right), \tag{2.18}$$

where the λ_n are the roots to $J_1(\lambda_n) = 0$, $m_n = \lambda_n/a$ and $\tau_n = (\tanh Bm_n)/Bm_n$. We have added the last term to take care of the non-slip condition. Although (2.18) represents the solution for our experimental situation, some insight can be gained by studying problems where lateral boundaries are absent and boundary conditions are imposed only along the bottom and the top. We turn our attention now to two simple cases.

3. Two simple solutions

The solution for a general distribution of horizontal velocities along bottom and top boundaries of infinite horizontal extent has been presented by Walin (1969). We shall look into the properties of two particular solutions of that general class because most of the results of the spin-up of fluid in a cylindrical container can be understood in terms of the behaviour of these two special flows. We first present the response of the fluid to simple harmonic forcing at the top and bottom. This gives information about the spin-up time and the penetration into the fluid of the effects of the boundaries. The second case involves a forcing which simulates that of the experiment but again lateral walls are absent. This gives us a picture of the effect of an abrupt spatial variation in the forcing at the top and bottom boundaries. In both cases we compare the results for stratified and homogeneous flow.

Harmonic forcing

Consider the case where the fluid is confined between infinite plates at $z = \pm 1$ and the boundary conditions on the velocities at $z = \pm 1$ are

$$\left.\begin{aligned} u &= -(l/k)\cos kx \sin ly\, H(t), \\ v &= \sin kx \cos ly\, H(t), \end{aligned}\right\} \tag{3.1}$$

where $$H(t) = \begin{Bmatrix}0\\1\end{Bmatrix} \quad \text{for} \quad t \lessgtr 0.$$

Initially the fluid is at rest in the rotating frame so that all dependent variables vanish for $t \leqslant 0$. Then (2.14) can be integrated with respect to time and we have

$$\nabla_H^2 p_0 + (1/B^2)\,\partial^2 p_0/\partial z^2 = 0. \tag{3.2}$$

The problem defined by (3.2) together with the boundary conditions (2.15) and boundary velocities specified by (3.1) is straightforward and the solution for p_0 is

$$p_0 = 2\frac{\cosh BKz}{k\cosh BK}\cos kx \cos ly\,(e^{-t/\tau}-1)\,H(t), \tag{3.3}$$

where $K^2 = k^2+l^2$ and $$\tau = (\tanh BK)/BK. \tag{3.4}$$

The pertinent information for our purposes is present even in the two-dimensional case ($l = 0$, $k = K$). For this simple flow the remaining variables are

$$\rho_0 = -\frac{\sinh BKz}{\cosh BK}\cos Kx\,(e^{-t/\tau}-1), \tag{3.5}$$

$$v_0 = -\frac{\cosh BKz}{\cosh BK}\sin Kx\,(e^{-t/\tau}-1), \tag{3.6}$$

$$\tilde{u}_0 = \sin Kx \sin\zeta\, e^{-\zeta} e^{-t/\tau}, \tag{3.7}$$

$$\tilde{v}_0 = \sin Kx \cos\zeta\, e^{-\zeta} e^{-t/\tau}, \tag{3.8}$$

$$w_1 = \frac{K\sinh BKz}{2\sinh BK}\cos Kx\, e^{-t/\tau}, \tag{3.9}$$

and $$u_1 = -\frac{BK\cosh BKz}{2\sinh BK}\sin Kx\, e^{-t/\tau}, \tag{3.10}$$

where $\zeta = (1-|z|)\,E^{-\frac{1}{2}}$, and the tilde variables are in the Ekman layer.

Hence, measured in units of $\Omega^{-1}E^{-\frac{1}{2}}$, the spin-up time for the present problem is given by (3.4). For every weak stratification ($B \ll 1$) we see from (3.4) that $\tau \to 1$. For very strong stratification ($B \gg 1$) the spin-up time tends toward $(BK)^{-1}$. If the total wave-number K is either large or small, the interpretation of the results must be adjusted accordingly since τ depends on the product BK.

The spatial dependence of v_0 also reflects the very different response of the fluid for small and large values of BK. For $BK \ll 1$ the entire column of fluid responds to the velocities imposed at the boundaries, whereas for $BK \gg 1$ the fluid in the immediate vicinity of the boundary is spun up in time τ but fluid in the middle layers will feel the effect of the boundaries on a time scale determined by diffusion.

The spin-up of the interior is brought about by the $O(E^{\frac{1}{2}})$ circulation given by u_1 and w_1. The stream function corresponding to (u_1, w_1) is

$$\psi_1 = -(\sinh BKz/\sinh BK)\sin Kx\, e^{-t/\tau}. \tag{3.11}$$

For $K = 1$ we plot the streamlines for $B \ll 1$ in figure 1 (*a*) and $B \gg 1$ in figure 1 (*b*). It is evident that for strong stratification the $O(E^{\frac{1}{2}})$ circulation does not penetrate very deeply into the interior and the fluid leaves or enters the boundary layer at a sharp angle to the horizontal. For very weak stratification the response is essentially that of a homogeneous fluid.

The foregoing results can be described in terms of simple physical processes. Consider, for example, the response of a strongly stratified fluid near the bottom boundary in the region where the Ekman boundary layer sucks fluid from the interior. The required downward flow will carry fluid of lower density past a point just above the boundary layer so that the density at that point will decrease with time. Accordingly, because of hydrostatic balance the local vertical pressure gradient will increase with time. Suppose that at a short distance to the left the Ekman suction is greater. Then the corresponding vertical pressure gradient will show a larger increase with time. At the middle level of a vertically

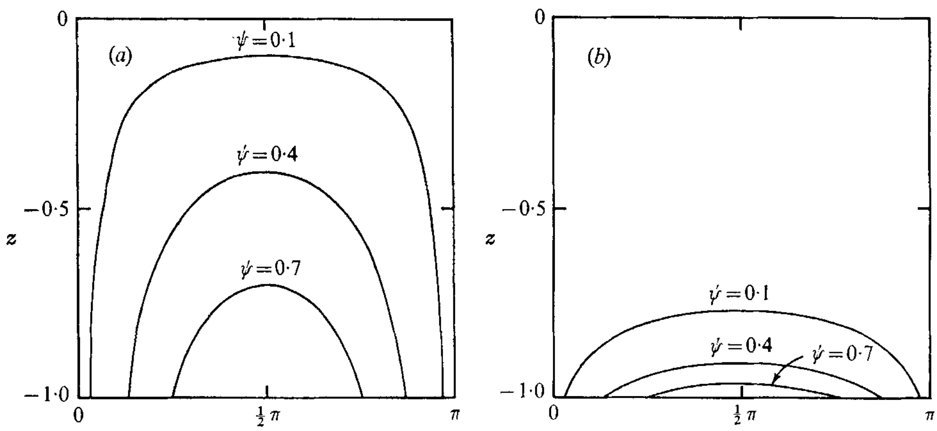

FIGURE 1. Reduced stream function, $\psi = \psi_1/e^{-t/\tau}$, with harmonic forcing. (*a*) $K = 1, B \ll 1$ $(B = 0)$. (*b*) $K = 1, B \gg 1$ $(B = 10)$.

symmetric system the pressure is constant. Hence, the net result at the level under consideration is a positive horizontal pressure gradient which increases with time, and, because of geostrophy, an acceleration normal to the horizontal pressure gradient will be generated. The Coriolis acceleration is balanced by a local acceleration, i.e. a flow to the left, which closes the vertical circulation pattern for the flow required by the Ekman motion conditions. This circulation continues until the redistribution of density and the associated geostrophic flow are compatible with the required values at the boundaries. The vertical circulation ceases and the fluid is then said to be spun up.

It is now clear why stratification shortens the spin-up time and why the whole process is limited to a region near the boundary. For a given magnitude of Ekman suction the local rate of change of the density perturbation will be larger the larger the basic stratification. Hence, the associated pressure gradients and velocities will also be greater and the spin-up will occur faster. For the same reason the vertical pressure gradients which are established near the boundary will be more quickly relaxed by the generated cross flow and the effects of Ekman suction will penetrate less deeply into the fluid. The latter effect is reflected also in the sharp angles with which the streamlines in figure 1 (*b*) meet the boundary and in the generally flattened streamlines.

When the stratification is moderate ($B \sim 1$) but the horizontal wavelength is small ($K \gg 1$), the spin-up time and the depth of penetration of the boundary effects are limited just as they are for $B \gg 1$ and $K \sim 1$. Even though the magnitude of the cross flow is much smaller than it is for $B \gg 1$, the horizontal distance over which the fluid must travel in order to re-establish the original stratification is much smaller and the net effect is the same as for $B \gg 1$, $K \sim 1$. A difference in detail for this case is that the $O(E^{\frac{1}{2}})$ streamlines intersect the boundary just as they do in figure 1 (*a*). In fact, the general streamline pattern is identical to that of figure 1 (*a*) but the level $z = 0$ must now be placed at a distance of $O(K)$ above the boundary $z = -1$.

For the case $B \sim 1$, $K \ll 1$ the fluid tends to respond as a homogeneous fluid. As we noted earlier, a particle leaves the bottom boundary layer of a stratified fluid, travels upward and horizontally and eventually turns downward again. If the horizontal scale is very large, the effect of the top boundary is felt by the fluid particle long before it is to turn down again and after that point the effect of stratification is no longer pertinent. Hence, if the forcing has a sufficiently large horizontal scale even a strongly stratified fluid will respond as a homogeneous fluid. (This point is particularly pertinent for large-scale flows in the ocean.)

We note that in dimensional terms the spin-up time is

$$t_{\text{spin-up}} = (\tanh BK/BK)\, L/(\nu\Omega)^{\frac{1}{2}}, \tag{3.12}$$

i.e. the spin-up time has a form indentical to that of the homogeneous system if we replace the vertical scale L by the stratification scale $L_s \equiv L \tanh BK/BK$. For the case of $BK \gg 1$, $L_s \approx L/BK$ and the spin-up time can be interpreted in terms of the homogeneous spin-up time if the Ekman number is defined in terms of the penetration depth instead of the total depth. Walin first pointed out this interpretation.

In the discussion of the experimental results for the cylindrical problem it will help to keep in mind the following features of spin-up as suggested by the simple example presented above: (*a*) When the fluid is spun up the azimuthal velocity of fluid close to the top and bottom boundaries will be the same as the imposed boundary velocities. Fluid near mid-depth will continue to move relative to the container until diffusion effects penetrate the interior. Hence, during spin-up the azimuthal displacement relative to the container will increase with distance from $z = \pm 1$. (*b*) When $B \gg 1$ only a thin layer of fluid will achieve the boundary velocity when the spin-up process (as we have defined it) is complete. (*c*) The spin-up time is shorter the larger the value of B.

Spatially non-uniform forcing

In the spin-up of a stratified fluid contained in a right cylinder with horizontal boundaries at the top and bottom the difference in azimuthal velocity between the interior fluid and the top and bottom boundaries is linear in the radial coordinate at the initial instant. After a time of $O(\Omega^{-1})$ the Ekman layers will have been more or less established and the fluid in the immediate vicinity of the lateral boundaries will have felt the influence of the side boundaries because of viscous diffusion. Hence, the difference in azimuthal velocity between the interior fluid and the top and bottom boundaries will be proportional to the radius but there will be an abrupt drop to zero at the cylindrical wall. The additional effects of the cylindrical wall serve to complicate the problem. In order to avoid these complications for the time being we treat the two-dimensional spin-up problem for the case where the top and bottom boundaries in the range $0 \leqslant x \leqslant 1$ are impulsively given the velocity $x - e^{(x-1)a}$, $a \gg 1$, at $t = 0$. We imagine that this velocity pattern is anti-symmetric about $x = 0$ and $x = \pm N$ $(N = 1, 2, 3, \ldots)$. Thus we avoid the additional effects of the side boundaries and concentrate only on the effect of the abrupt change in the velocity profile.

The mathematical problem can be solved by imagining that the boundaries are fixed and the interior fluid initially has the velocity $-x + e^{(x-1)a}$ in the range $0 \leqslant x \leqslant 1$. It is more convenient to treat the cylindrical problem in this fashion and we therefore solve the present problem in the same way. In addition to (2.23) we have

$$v_0 = -x + e^{(x-1)a} \quad \text{at} \quad t = 0, \tag{3.13}$$

and the boundary conditions

$$u = v = w = 0 \quad \text{at} \quad z = \pm 1. \tag{3.14}$$

The solution is obtained by a straightforward procedure and the pertinent results for our discussion are the zonal velocity,

$$v_0 = -x + e^{(x-1)a} + \frac{2a^2}{\pi} \sum_{m=1}^{\infty} \frac{(-)^m \sin m\pi x}{m(a^2 + m^2\pi^2)} \frac{\cosh Bm\pi z}{\cosh Bm\pi} (e^{-\lambda_m t} - 1), \tag{3.15}$$

and the stream function ψ for the (u_1, w_1) field,

$$\psi = \frac{a^2}{\pi} \sum_{m=1}^{\infty} \frac{(-)^m \sin m\pi x}{m(a^2 + m^2\pi^2)} \frac{\sinh Bm\pi z}{\sinh Bm\pi} e^{-\lambda_m t}, \tag{3.16}$$

where

$$\lambda_m = \frac{Bm\pi}{\tanh Bm\pi}. \tag{3.17}$$

This solution involves an error of e^{-a} in the value of v_0 at $x = 0$ but since we take $a \gg 1$ the error is negligible.

In figure 2(*a*) we show $-v_0$ at $t = 0$ for the range $0 \leqslant x \leqslant 1$ as given by (3.13) with $a = 100$. This profile is linear in x with an abrupt decrease to zero near $x = 1$. Also shown in figure 2(*a*) is the $-v_0$ profile for $B = 0$ (a homogeneous fluid) at $t = 1$, i.e. after a time interval corresponding to a spin-up time for a homogeneous fluid. We observe that $-v_0$ keeps the same spatial structure but the amplitude is decreased by the factor e^{-1}.

Profiles of $-v_0$ for a stratified fluid with $B = 1$ are shown in figure 2(*b*). At $t = 1$ the profile at the middle level, $z = 0$, shows little change from the original profile. As we noted earlier, at the middle level the larger scales are affected more strongly than the smaller scales by the viscous processes in the Ekman layers. The originally linear part of the $-v_0$ profile is now slightly concave because at mid-level the largest effect of spin-up comes from the largest mode, which vanishes at $x = 0, 1$ and has a maximum in the middle. Hence, relative to the original velocity profile the strongest spin-up is manifested at $x \approx \frac{1}{2}$. The region of abrupt variation near $x = 1$ is essentially unaffected by the spin-up process because the scale of variation is small and for these scales the effects of the Ekman layers are confined to regions closer to the top and bottom boundaries.

We note from figure 2(*b*) that at $z = -1$, i.e. just outside the Ekman layer near the bottom boundary, the fluid is nearly completely spun up at $t = 1$. At this level all scales are affected by the spin-up process. Furthermore, as we noted earlier, the smaller scales are spun up in a much shorter time than the larger scales. Hence, the small-scale structure of the original v_0 profile is no longer present and v_0 is practically symmetric about $x = \frac{1}{2}$.

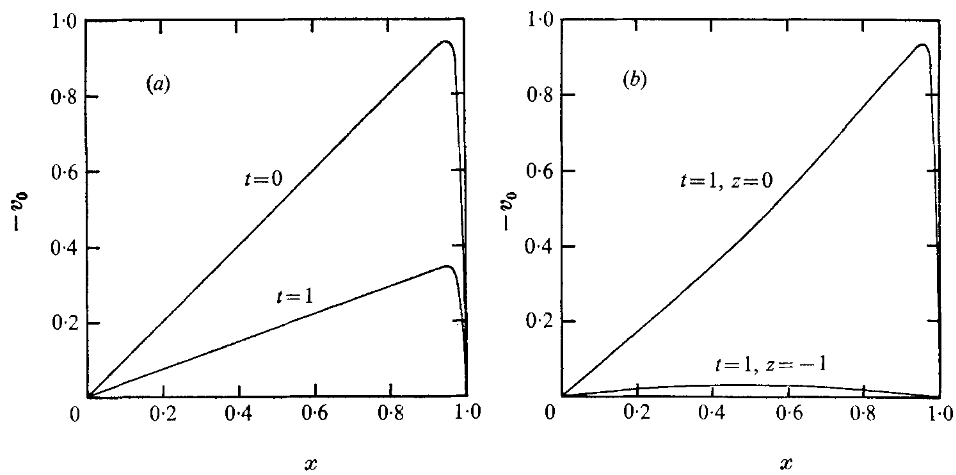

FIGURE 2. Zonal velocity, v_0, with spatially non-uniform forcing ($a = 100$) for (*a*) $B = 0$ and (*b*) $B = 1$.

Contours of the stream function for the meridional circulation (the (u_1, w_1) field) are shown in figures 3 and 4 for the cases $B = 0$ and $B = 1$, respectively. In figure 3 the flow for the homogeneous fluid at $t = 0$ corresponds to the circulation which is set up after the Ekman layer has been established. The streamline pattern shows the fluid rising in the narrow boundary region and falling in the broad interior region. At $t = 1$ the flow pattern has the same spatial form but the amplitude of ψ is decreased to e^{-1} of its original value.

The remarkable change in the meriodional circulation wrought by the stratification ($B = 1$) is evident in figure 4. Initially the circulation set up by the Ekman layer shows a concentration of streamlines toward $x = 1$ in the vicinity of the boundary but higher up the flow is more nearly symmetric about $x = \frac{1}{2}$. This tendency toward symmetry again reflects the penetration of only the larger scales to the middle levels of the fluid. At $t = 1$ the asymmetry of the streamline pattern near $z = -1$ has largely vanished and the entire pattern now shows a nearly symmetrical structure about $x = \frac{1}{2}$. The dashed curve in each figure marks the transition region from upward to downward flow. The stream function in figure 4 has a much smaller amplitude than that of figure 3. This reflects the faster spin-up time for the stratified fluid.

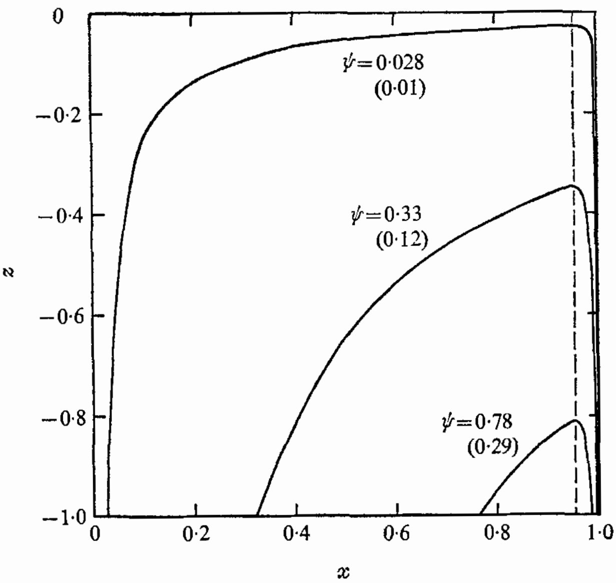

FIGURE 3. Stream function, ψ, with spatially non-uniform forcing (a = 100) for $B = 0$ at $t = 0$ and $t = 1$. The stream function at $t = 1$ (the value in parentheses) is decreased to $1/e$ of its original value.

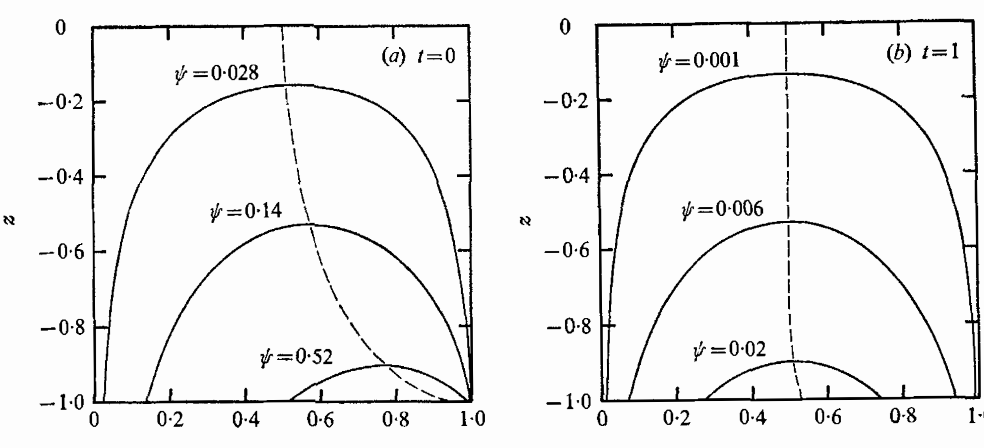

FIGURE 4. Stream function, ψ, with spatially non-uniform forcing (a = 100) for $B = 1$ at (a) $t = 0$ and (b) $t = 1$.

4. Experimental apparatus and procedure

Experiments were performed on a rotating table driven by a synchronous motor through a Graham variable speed transmission. The fractional deviation of the rotation rate was less than $\pm\ 4 \times 10^{-4}$ on the time scale of the experiment, and this variation was primarily due to the imperfections in the timing belt and geared pulley combination which couples the table to the transmission. The axis of rotation was aligned within 5 sec of arc with the vertical (gravitational field).

The working fluid, distilled water stratified with NaCl, was contained in a clear 0·64 cm thick Plexiglas cylinder, 19·0 cm in diameter and 12·1 cm in height, with a rigid 0·64 cm top cover. The test container was placed on a 2·5 cm thick piece of Phenolic and covered with another 0·64 cm thick Plexiglas cylinder so that a 0·64 cm air gap separated the two containers at the walls and top surface. The second container and the air gap were used to dampen the room temperature fluctuations and drift during the course of the experiment. The flow in the container was photographed with a camera mounted on the rotating table above the container and coincident with the axis of rotation. Photographs were taken at selected intervals and the time was recorded by a stop watch ($\frac{1}{5}$ sec resolution) mounted adjacent to the container.

The stratified fluid was prepared by the 'slip-under method' (Fortuin 1960), used in the preparation of density gradient columns. In brief, an open tube is connected to the bottom of two tanks, one with pure water and the other with salt water of desired density. As the pure water tank is slowly drained, salt water enters and is mixed with the fresher water with the aid of a stirrer. Thus, the fluid in the mixing tank, originally containing pure water, becomes saltier with time. The drained fluid is fed into the test container through a hole in the bottom edge of the container; the incoming denser fluid displaces the less dense fluid introduced previously. In this way, a nearly linear density gradient is obtained. The linearity of the gradient depends on the rate of flow from the mixing tank and the thoroughness of the mixing process. Two to four hours are generally required to successfully complete the filling of the test container. The container was filled while the turn-table was rotating but the supply tanks were in the laboratory frame.

The density gradient in the container was inferred from the density of pure water at the top, the positions of calibrated density floats in the interior of the fluid, and the density at the bottom of the container. The latter was assumed to be the same as the density of the fluid remaining in the mixing tank at the completion of the filling process. The density of the fluid in the mixing tank was read with a hydrometer which had been calibrated with solutions of known density. The calibrated density floats, approximately 4 mm in diameter, were introduced into the fluid at the conclusion of the spin-up experiment and the vertical position was read with a cathetometer while the container was still rotating at the final rotation rate. A representative density gradient is shown in figure 5 (experiment SS14). The straight line represents the gradients used in the calculations.

After the container is filled with the stratified fluid, approximately 2 h are required before the experiment can begin. As a consequence of the filling procedure, a strong asymmetric flow is present in the container and the fluid must be allowed to reach a state of rigid-body rotation.

Observations and measurements of the spin-up flow field were made by photographically following a neutrally buoyant dyed parcel of fluid. The dye was produced by the Thymol Blue pH indicator technique described by Baker (1966). The method consists of placing fine wire electrodes in the pH indicator solution which has been titrated to the end point. An electric current is allowed to flow momentarily between the electrodes. The pH of the solution near the negative electrode changes and the colour of the solution in the immediate vicinity of the electrode changes accordingly. The resulting dyed fluid is neutrally buoyant.

In our experiments, platinum + 10 % irridium wires 0·005 cm in diameter served as the negative electrodes and were strung across the diameter of the container. The positive electrode was a short stub, approximately one centimetre in length, of the same wire and located near the negative electrodes. The arrangement of using a short stub of wire for the positive electrode avoids the formation of bubbles and irregular sheets of dye about the negative electrodes in

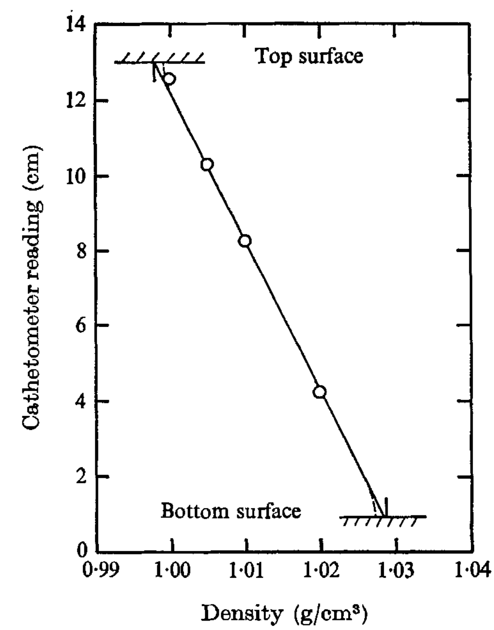

FIGURE 5. A representative density gradient, $B = 0{\cdot}708$ (experiment SS 14).

the strongly conducting fluid. After a solid cylinder of dye was formed the rotation of the table was changed and the first photograph taken at this time, i.e. while the dial controlling the output rotation of the Graham transmission was being changed. The time taken to change the rotation was approximately one second. The centre of a dye line at a given radius was taken as the point representing the parcel of fluid being followed. The rate of change of the angular position of the marked fluid as a function of time represents the raw data of the experiment.

The meridional flow field was observed by viewing the vertical distortion of the dye lines, i.e. by viewing the container from the side. The cylindrical container was placed in a square Plexiglas container and the space between containers was filled with water. This arrangement permits one to view the edge of the cylindrical container without distortion. The camera was mounted in the plane of the table. Two wires were used at 0·5 and 1·0 cm above the bottom boundary. The plane of the wires was inclined at approximately 30° to the plane of the camera.

Several stratified spin-up experiments were also conducted by using neutrally buoyant spheres. The results of these experiments were essentially similar to those obtained with the wire technique. At mid-level the results of the two methods could not be distinguished quantitatively. The neutrally buoyant float method, however, introduces more uncertainties near the horizontal boundaries and in general provides less information per experiment than does the pH indicator technique. For this reason, the neutrally buoyant float experiments were not pursued.

5. Qualitative discussion of the experimental results

This section contains a description of those features of the stratified spin-up experiments that could be observed by the present techniques. We shall refer to specific experiments to illustrate the particular phenomenon under discussion. The data for the different experiments are summarized in table 1.

Experiment number	B	ρ bottom $-\rho$ top (g/cm^3)	Ω (rad/sec)	$\frac{\Delta\Omega}{\Omega}$	a	τ_h (sec)
SS 14	0·708	0·0303	1·101	0·0134	1·57	58·0
SS 24	0·456	0·0454	2·034	0·0104	1·49	44·8
SS 27	1·44	0·130	1·099	0·0116	1·57	56·0
SS 31	0·684	0·0287	1·110	0·0209	1·57	57·7

TABLE 1. Summary of experimental parameters

Rigid-body rotation

Spin-up is defined as the process of fluid adjustment which occurs when the rotation rate of the container is increased abruptly from one value to a slightly larger value. The fluid is assumed to be in a state of a rigid-body rotation prior to spin-up. Such a state is not possible for a rotating stratified fluid, however, because the pressure surfaces that accompany a state of rigid-body rotation are paraboloids of revolution and the density surfaces cannot be parallel to the pressure surfaces because of diffusive processes. Hence, a relative flow, referred to as the Sweet–Eddington (SE) flow, will exist. In order to determine the intensity of the SE flow the following procedure was adopted.

Prior to spin-up the system was observed, via dye lines in the fluid, over a period of time comparable to the duration of the spin-up experiment which was to follow. When the initial rotation rate was no larger than 1 rad/sec, the aximuthal displacement of the dye line (observed to be a maximum near mid-radius) was less than 1 to 2 degrees at $z = -0{\cdot}8$ and practically not noticeable at $z = 0$. At rotation rates of 2 rad/sec and higher the azimuthal displacement of the dye line in the SE flow was not negligible compared with the total displacement of the line during the spin-up experiment. For example, the SE displacement at the level $z = -0{\cdot}84$ for experiment SS 24 (performed at 2 rad/sec) prior to spin-up is shown in figure 6 along with the displacement observed during the actual spin-up experiment which followed. The SE displacement is largest near the bottom boundary. At mid-level the displacement is in the same direction but of considerably smaller magnitude (of the order of one degree at the end of three minutes) and for this reason is not shown. Experiments at rotation rates of 3 rad/sec were abandoned due to the strong SE flow. Although SE flow is always present to some extent in the experiments, we shall use the term 'rigid-body rotation' as the flow in the absence of spin-up.

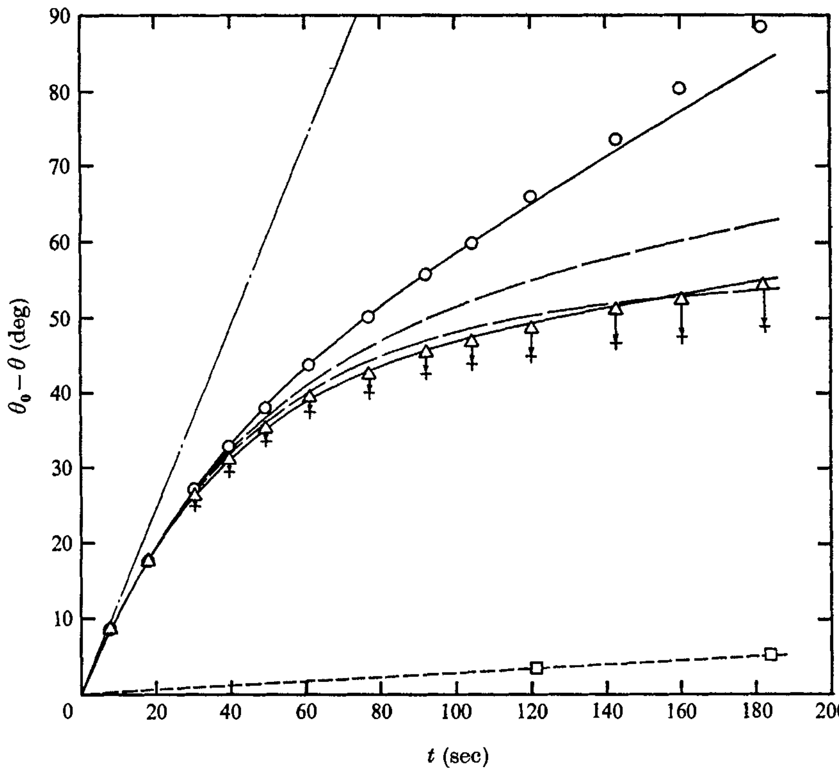

FIGURE 6. The azimuthal displacement field as a function of time for $B = 0{\cdot}456$ and $\Delta\Omega/\Omega = 0{\cdot}010$. ○, △, experiment (SS 24) at $z = -0{\cdot}055$ and $r/a = 0{\cdot}493$, and $z = -0{\cdot}843$ and $r/a = 0{\cdot}515$, respectively; ———, Walin (1969); — —, Holton (1965); □, experimental measurement of the Sweet–Eddington flow at $z = -0{\cdot}843$, prior to the change in rotation rate; +, an approximation of the displacement field at $z = -0{\cdot}843$ in the absence of the Sweet–Eddington flow.

Spin-up time at a point in the fluid

After the rotation rate of the container is increased abruptly, the fluid velocity at each point will change from its initial value to a final value. From the data showing azimuthal displacement $\Delta\theta$ *vs.* time t at given values of r and z (two of these are shown in figure 6) the velocity of the fluid at any time can be estimated from the slope of the 'best' curve through the experimental points. The initial velocity is given by the change in the rotation rate (the slope of the curve at the initial time) and the final velocity is obtained from the slope of the curve through the last few points. Because the curve is monotonic there is one value of time

τ when the velocity differences between $t = 0$ and $t = \tau$ is $1/e$ of the differences between initial and final velocities. This is defined as the spin-up time. The spin-up time was determined for experiments with $0{\cdot}4 \leqslant B \leqslant 1{\cdot}4$, corresponding to rotation rates of 1 to 2 rad/sec and total density differences between top and bottom of 3 % to 12 %. The Ekman number for these experiments was between 10^{-4} and 3×10^{-4} while the Rossby number, the measure of the change in rotation rate, was kept between 0·01 and 0·015. Determinations of τ as a function of B

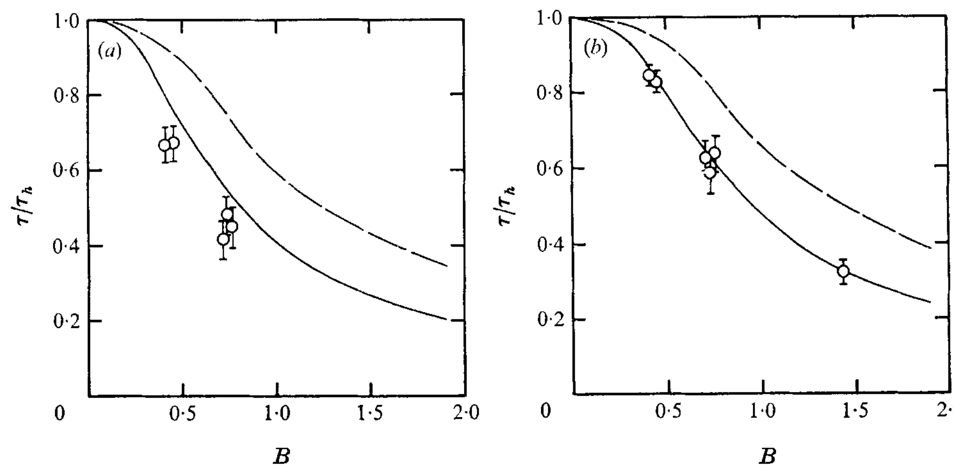

FIGURE 7. The ratio of stratified to homogeneous spin-up times, τ/τ_h, as a function of the parameter B with $a = 1{\cdot}5$ to $1{\cdot}6$, and $r/a = 0{\cdot}5$. ○, experiment; ———, Walin (1969); —— —— ——, Holton (1965). (*a*) $z = 0$, and (*b*) $z = -0{\cdot}8$.

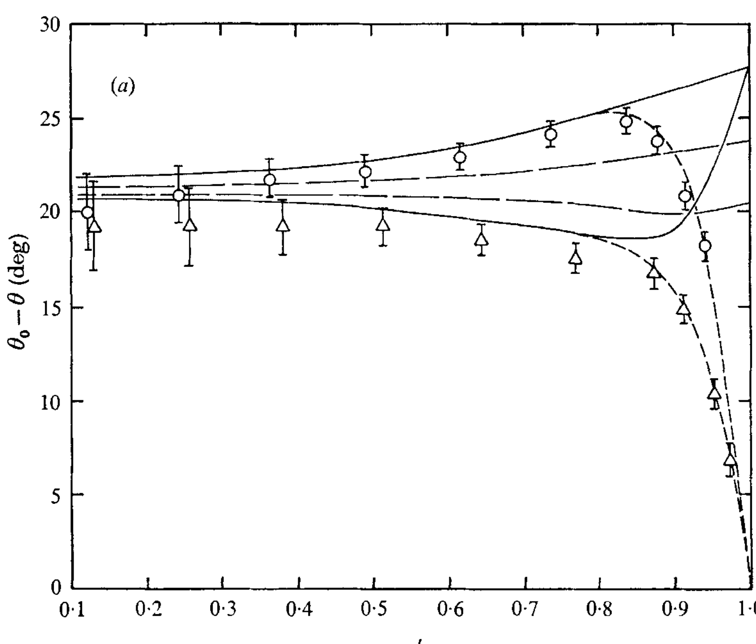

FIGURE 8(*a*). For legend see facing page.

near mid-level and near the bottom boundary are shown in figure 7. The error bars over the experimental points indicate the uncertainty in selecting the point at which the slope corresponds to the velocity characteristics of the spin-up time.

The results in figure 7 demonstrate the qualitative behaviour predicted by the simple harmonic solution, equation (3.12); i.e. τ is shorter for larger B and approaches the spin-up time for a homogeneous fluid as $B \rightarrow 0$.

Azimuthal displacement vs. radius and time

Measurements of azimuthal displacement ($\Delta\theta$) as a function of radius r/a are shown in figures 8 (*a*) and 8 (*b*) for experiment SS 14 at 32·8 and 126·4 sec respectively after the initiation of the spin-up process. Error bars over the symbols denoting experimental measurements represent the arc subtended by the marked fluid and the maximum error in reading the displacement from the photographs.

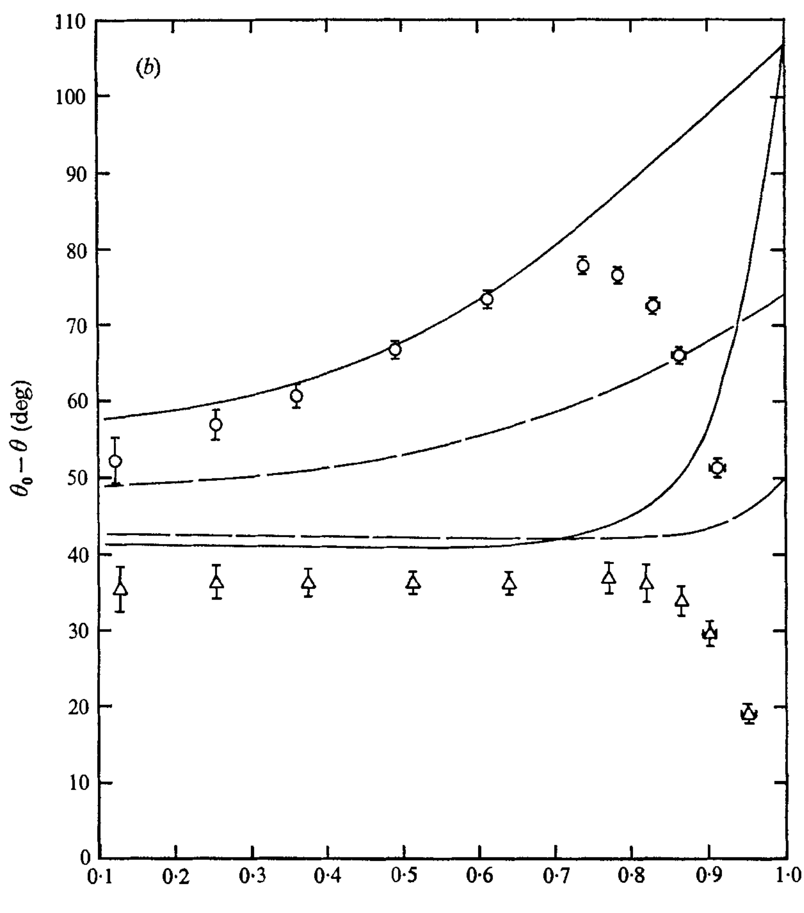

FIGURE 8. The azimuthal displacement field as a function of radius, r/a, for $B = 0{\cdot}708$ and $\Delta\Omega/\Omega = 0{\cdot}013$. ○, △, experiment (SS 14) at $z = -0{\cdot}005$ and $z = -0{\cdot}834$, respectively; ———, Walin (1969); ——— ———, Holton (1965). (*a*) After 32·8 sec. The effects of lateral diffusion on Walin's theoretical curves are shown as dashed curves in the region $0{\cdot}8 \leqslant r/a \leqslant 1$. (*b*) After 126·4 sec.

It is evident from these two figures that the $\Delta\theta$ *vs.* r curves differ from level to level. Hence, the azimuthal flow field can be synthesized from a number of curves generated at different levels. A qualitative picture of the azimuthal flow field 61 sec after spin-up for experiment SS 31 can be obtained from dye lines at four levels ($z = -0{\cdot}005$, $-0{\cdot}58$, $-0{\cdot}83$ and $-0{\cdot}92$) and originally generated along the diameter shown by the dashed line in figure 9 (plate 1). In the experiments for which quantitative data were taken only two wires, strung perpendicular to each other at two different levels, were used. This arrangement separates the dye lines and permits more accurate measurement of displacement.

The interpretation of the radial behaviour of the azimuthal velocity is facilitated by the solution of the spatially non-uniform forcing example. This example is relevant in that the initial velocity in a spin-up experiment is also linear except for a small region affected by the wall. At the moment of spin-up and during the first few seconds of the flow the dye lines at all levels appear linear and of the same magnitude in angular displacement. In a very narrow region near the wall, as the fluid moves relative to the container, the dye line is stretched out from its point of contact with the wall to the point of tangency with the original straight line. As the flow progresses, the narrow diffusive region penetrates deeper into the interior. At the same time dye lines at lower levels are retarded as spin-up is achieved.

The behaviour described above is represented in figure 9, where dye lines at four levels are shown. Let us focus particular attention at the two extreme levels and view them with the non-uniform forcing solution in mind. The sharp variation of the velocity field near the wall is a small-scale phenomenon and we have observed in the simple examples that for such small scales the effects of the Ekman layers do not penetrate far from the top or bottom boundaries. Furthermore, the smaller scales respond to spin-up in a much shorter time than do the larger scales. Hence, the displacements are much smaller at the lower level and the curvature of the dye line is also less. The larger curvature at mid-level reflects the smaller effect (particularly with respect to smaller scales) of the spin-up processes at that level. Furthermore, the displacement of the dye at mid-level is only mildly affected by Ekman layer processes with the greatest effect in the vicinity of $r/a = \frac{1}{2}$. Although this effect is present in the photograph, it is more directly observed in the displacement *vs.* radius curve of figure 8(*b*) for a similar experiment. In terms of absolute displacement, $(r/a)\Delta\theta$, the maximum retardation does, indeed, take place near $r/a = \frac{1}{2}$ ($r/a = 0{\cdot}5$ to $0{\cdot}6$ for experiment SS 14). Retardation here is measured relative to the position that the fluid would occupy in the absence of spin-up flow. At the time of the photograph, the effect of diffusion has penetrated to a point about a third of the radius in from the wall.

The time dependence of the azimuthal displacement field is also in clear agreement with the theoretical examples. All experimental results given as a function of time demonstrate that the final state of the fluid is not one of rigid-body rotation, as is the case for a homogeneous fluid, but rather a state of quasi-steady flow on the spin-up time scale. When azimuthal displacement is plotted against time, figure 10, the experimental measurements show a linear relationship with time after several spin-up times, and the slope is non-zero. The initial velocity is represented everywhere by the slope of a line through the origin.

The experimental data presented above do not extend beyond approximately 4 min since on this time scale the terminal velocity becomes steady. However, as one continues to observe the flow beyond this time, the displacement with time begins to diminish again and rigid-body rotation is achieved within 2–3 h, i.e. after a diffusion time. One need not wait beyond 4 min to observe the effects of diffusion, however, as the fluid near a wall will sense diffusion at a much earlier time. For this reason the experimental displacement–time data is presented at $r/a \approx \frac{1}{2}$. At larger values of r diffusion effects begin to obstruct the pure spin-up response.

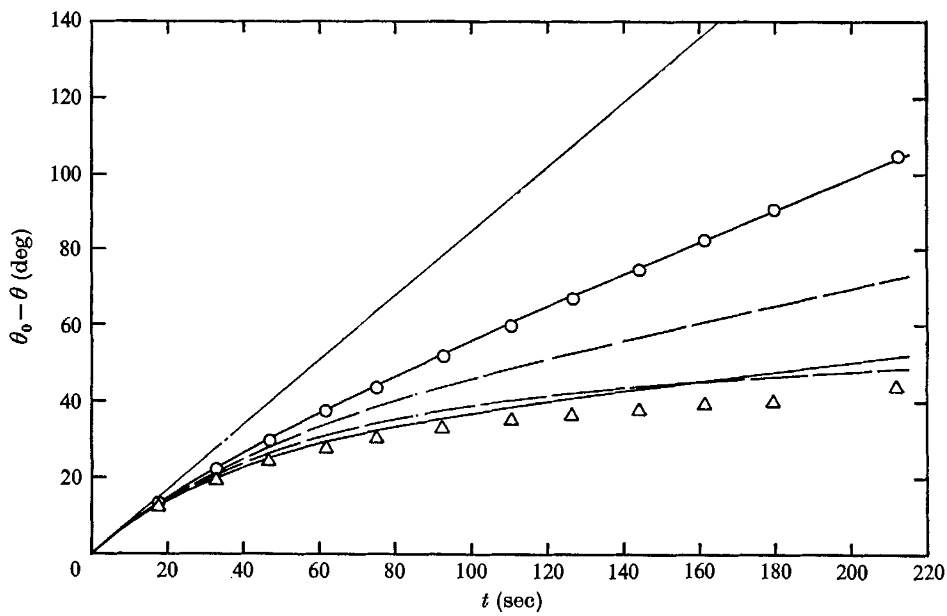

FIGURE 10. The azimuthal displacement field as a function of time for $B = 0{\cdot}708$ and $\Delta\Omega/\Omega = 0{\cdot}013$. ○, △, experiment (SS 14) at $z = -0{\cdot}005$ and $r/a = 0{\cdot}492$, and $z = -0{\cdot}834$ and $r/a = 0{\cdot}515$, respectively; ———, Walin (1969); — — —, Holton (1965).

The behaviour of the azimuthal velocity as a function of stratification and height above the bottom boundary is also clearly demonstrated by the displacement–time data. Fluid spin-up is strongest near the bottom boundary for a given stratification. With increasing stratification spin-up is confined to a thinner region near the boundary. Hence, the terminal slopes are larger (i.e. closer to the initial slope) at mid-level for a given stratification, and the terminal slopes are also larger for a larger stratification at a given level. Figures 6, 10 and 11 show the effect of increased stratification. Only the layer of fluid above the Ekman layer reaches rigid-body rotation. Although measurement of the flow at this level was not made, this behaviour was easily observed with dye. Crystals of dye were dropped into the container prior to spin-up so that a trail of dye extended from the top of the container to the crystal at the bottom. Just after the initial instant the entire trail of dye was observed to move. After a few minutes of the flow, however, the dyed fluid near the bottom of the container came to relative rest while the fluid above continued to move. The velocity of the moving fluid increased upward to the mid-level of the tank.

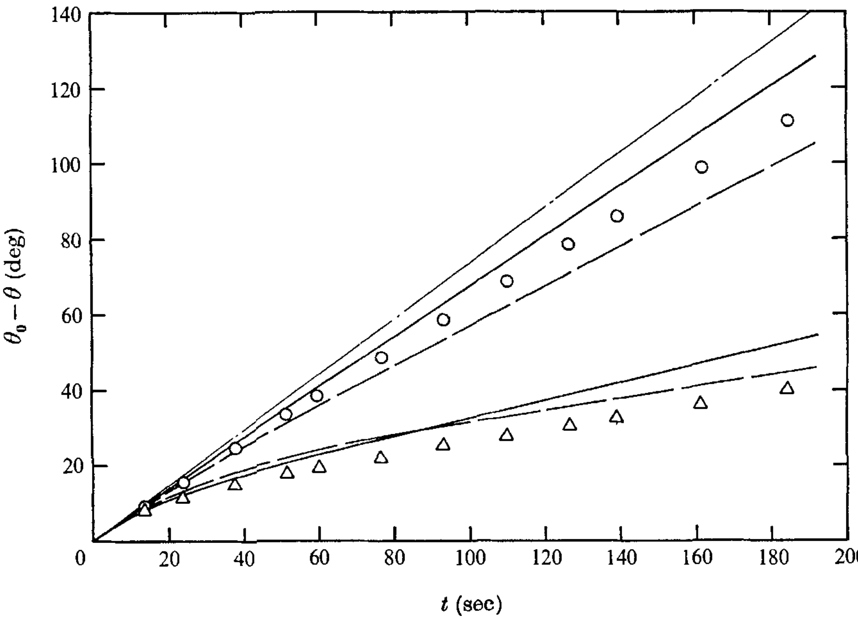

FIGURE 11. The azimuthal displacement field as a function of time for $B = 1{\cdot}44$ and $\Delta\Omega/\Omega = 0{\cdot}012$. ○, △, experiment (SS 27) at $z = -0{\cdot}005$ and $r/a = 0{\cdot}492$, and $z = -0{\cdot}834$ and $r/a = 0{\cdot}515$, respectively; ———, Walin (1969); — — —, Holton (1965).

Observations of meridional flow

Observations of the gross features of meridional flow were made for both homogeneous and stratified fluids by viewing the vertical displacement of a horizontal dye line from the side of the container. The results presented for homogeneous fluids are intended as an aid for the qualitative interpretation of the corresponding stratified flow.

As mentioned in §4 side photographs were taken of dye lines which were originally generated along a line inclined 30° to the normal plane of view of the camera. As time goes on, the dye lines rotate azimuthally. Hence, at some time a dye line in the interior of the fluid will be normal to the line of sight and at a still later time it will be parallel to the line of sight (and therefore appear as a point). The portion of the dye line that lies closer to the side wall will be stretched azimuthally from the point of contact with the wall to the point of tangency with the interior dye line (see figure 9 (plate 1) for a top view).

Side photographs of a homogeneous spin-up experiment are shown in figure 12(*a*) (plate 2). The photographs show the position of the dye at the initial instant and 63 sec after spin-up. The spin-up time τ_h is 62 sec, the final rotation rate 1·11 rad/sec, and the change in the rotation rate 1·9 %. This record will serve as a basis for evaluating the corresponding stratified spin-up record and is therefore considered first. Note that the fluid to the right of the rotation axis is flowing out of the plane of the photograph and to the left into the plane of the photograph, and that the original position of the dye line is at an angle to the line of sight, hence the difference in appearance of the dye near the walls. The sharp curvature of the dye line near the walls represents the upward flow in the side-wall boundary layers. Slight downward motion can also be detected in the interior of the fluid.

Side photographs of the corresponding stratified spin-up with $B = 0{\cdot}79$ are shown in figure 12(*b*). The initial position of the dye and the position 57 sec after spin-up are shown. The dimensionless stratified spin-up time τ_s/τ_h is approximately 0·59 at the level $z = -0{\cdot}8$, the rotation rate is 1·10 rad/sec and the change in rotation rate is 1·5 %. The strong upward motion near the wall detected in the corresponding homogeneous example is absent here. Although some vertical motion is present, it appears more evenly distributed along the particular level without sharp or distinct vertical motions. This observation confirms Pedlosky's conclusions that the radial transport of the Ekman layers at the horizontal boundaries cannot be accepted by side-wall boundary layers of the type encountered in a homogeneous fluid. The side-wall boundary layer is simply an $O(E^{\frac{1}{2}})$ layer which diffuses the azimuthal velocity of the wall into the fluid.

The meridional circulation can be intensified by increasing the rotation rate of the container by a larger amount. Side photographs of homogeneous spin-up with 7·3 % change in rotation rate are shown in figure 13(*a*) (plate 3). Photographs show dye positions at 0, 7 and 25 sec after the change in rotation rate. The spin-up time is 60 sec and the final rotation rate is 1·17 rad/sec.

In the interest of clarity, only the very early times of the flow are shown because the dye experiences large displacements due to the large initial velocity and interpretation at later times becomes difficult without simultaneous records of the flow from above. The stronger flow is evident here, in terms of the displacement both near the wall and in the interior. In the photograph taken 25 sec after spin-up, the dye in the interior region of the fluid is parallel with the line of sight. (The curved lines of dye in figure 13(*a*) are contained in the side boundary layer.) Before one spin-up time the lower dye line becomes absorbed in the Ekman layer where the horizontal flow is directed toward the wall.

The corresponding stratified spin-up was performed with the same fluid used above and approximately 1 h after the 1·5 % spin-up experiment. One hour between the consecutive experiments is sufficient for the flow field resulting from the 1·5 % spin-up to become negligible compared with the flow induced by a stronger spin-up. The increase in the rotation rate here is 11 % and the side photographs of the flow at 0, 4 and 17 sec after the change in rotation rate are shown in figure 13(*b*). The photograph after 17 sec shows the dye lines in the interior approximately parallel with the line of sight. The dye lines in this photograph have been touched up to make the dye appear darker.

The downward flow of fluid in the interior region appears similar in both the stratified and homogeneous spin-up flow; the character of the flow near the wall, however, once again appears significantly different. The structure in the side-wall boundary layer demonstrated by the homogeneous flow is not observed in the stratified flow. The stratified fluid shows a smaller but sharper rise next to the wall and a more gradual blending of the dye into the interior region than that observed in the homogeneous spin-up flow.

The difference in the magnitude of the actual vertical displacement of the dye between the homogeneous and stratified examples is not immediately apparent owing to the appreciable difference in the change in rotation rates. On close inspection of the photograph at 17 sec, however, one can detect that the lower dye line has reached the bottom boundary and that some of the dye is being carried laterally by the Ekman boundary layer toward the side wall, while in the corresponding homogeneous photograph after 25 sec the lower dye line in the interior had not yet reached the bottom boundary. The above conclusion is further substantiated by photographs at later times not shown here. The stronger (11 %) stratified spin-up flow example shows a stronger downward flow in the interior and a weaker but broader flow near the wall compared with the weaker (7·3 %) homogeneous spin-up flow example. It should be noted, however, that in the stratified spin-up experiments a large change in rotation rate, of the order of 10 % and larger, creates a weak instability in the Ekman boundary layer near the wall of the container. Instabilities are not observed in stratified spin-up experiments where the change in rotation rate is of the order of one per cent.

6. Comparison between theory and experiment

We shall now compare quantitative experimental results with the theoretical solutions to the problem by Holton (1965) and Walin (1969). Results of Sakurai's solution are not presented separately since they are identical to Walin's. Holton's theory is based on perfectly conducting side-wall boundaries. However, we include the comparison, because his experiments, used to compare with his theory, correspond to ours.

Consider first the azimuthal displacement as a function of time. Experimental results at mid-level and mid-radius for different values of B are shown in figures 6, 10 and 11 along with the theoretical predictions of Walin and Holton. Walin's displacement values lie consistently above Holton's and generally closer to the experimental values. With $B = 0{\cdot}71$, figure 10, the agreement between theory and experiment is remarkable. At a lower value of B, figure 6, the experimental measurements tend to become larger than the theoretical predictions at larger times. In figure 11, the experimental results fall approximately between the predicted displacements of the two theories. Disagreement between theory and experiment for this larger value of B is too large to be easily explained by experimental error. The more important experimental errors will be discussed in detail below. Here we mention only that errors due to wire drag and the nature of the response of the rotating table to an imposed change in the motor speed tend to reduce the experimental displacements by 3 % to 5 %.

Measurements made closer to the bottom boundary ($z = -0{\cdot}83$) show consistently smaller values than those predicted by theory. In both figures 10 and 11 there is a significant difference between theory and experiment and again the departure is too large to be attributed to experimental error. For small B, figure 6, the raw experimental points (triangles) seem to correspond very well to Walin's predicted values, but, when the Sweet–Eddington circulation is subtracted, the resulting values (crosses) show a departure from theory of about the same magnitude as in the other two experiments.

If we make use of the knowledge gained from the simple models in § 3, we can interpret the quantitative results as follows. At mid-level and mid-radius, effects from only the larger scales will manifest themselves. On the other hand, the most pronounced effect of spin-up occurs closer to the top and bottom boundaries and the smaller-scale processes are confined to these regions. Hence, it appears that Walin's theoretical analysis yields a more accurate description for the larger-scale motions than it does for the smaller-scale ones. It also tends to underestimate spin-up in the region where it is most concentrated. These conclusions are consistent with the approximations made in the theory. The relatively small scales in the region near the outer edge of the Ekman layer where the fluid must flow upward and radially inward cannot be treated analytically because non-linear effects must be important there. Hence, we can conclude that the processes which take place in the corner region must enhance the spin-up. Although based on indirect evidence, this conclusion should be a useful guide in treating the more complete problem.

The spin-up times can be determined from the curves showing displacement *vs.* time. These spin-up times are shown in figures 7 (*a*) and 7 (*b*) for the two levels $z = 0$ and $z = -0{\cdot}8$. Holton's theoretical values are much larger than the experimental ones. Walin's yield better agreement but it is interesting to note that his values at mid-level are larger than the experimental ones by an amount in excess of the reading error of the slopes of the curves. At the lower level the experimentally determined spin-up times agree very well with Walin's results. Hence, we are confronted with the paradox that theory and experiment yield a detailed time behaviour which is better at mid-level than in regions near the Ekman layer but the integrated result, represented as spin-up time, shows better agreement at the lower level. It is possible that the experimentally measured spin-up times are in error by an amount greater than indicated since small errors in displacement can have a corresponding large effect on the slope of the curve, particularly since a relatively small number of points defines the curve in the vicinity of the spin-up time. In general, spin-up time measurements are less reliable than the displacement measurements. It is noteworthy, however, that at mid-level the experimental measurements consistently fall below the theoretical prediction.

An alternative explanation for the above paradox may be based on the consequence of molecular diffusion of salt at the horizontal boundaries. During the several hours before spin-up, salt diffusion decreased the density gradient near the boundaries. This behaviour is described in greater detail in § 7. The weaker stratification near the boundaries may permit deeper penetration of the effects of the boundaries into the fluid, and hence produce a longer spin-up time and shorter displacement relative to the situation at mid-level where the density gradient has been undisturbed by diffusion. Consequently, the agreement in spin-up time between experiment and Walin's theory above the Ekman layer may be fortuitous! In the absence of distortion at this level, the spin-up time may be shorter and displacement larger. Unfortunately, the diffusion process and the long time required before an experiment can begin is inherent in the experimental method and cannot be realistically eliminated.

The radial variation of the azimuthal displacement is discussed only for the representative experiment at $B = 0{\cdot}71$. The behaviour for other values of B is essentially the same and will not add substantially to the present discussion. The displacement field at two levels is shown in figures 8(*a*) and 8(*b*), 32·8 sec and 126·4 sec, respectively, after spin-up. It is evident from these curves that agreement between theory and experiment is best at mid-radius. The results presented in figure 10 showing temporal variation of azimuthal displacement reflect this fact. The large discrepancy between theory and measurements near the wall can be eliminated by including the effects of diffusion of momentum from the side wall. In figure 8(*a*) we have included the term $v_0^{(\frac{1}{2})}$ from (2.18) to show the improvement that results near the side wall.

There is also disagreement between theory and experiment for small values of r at mid-level. Part of this discrepancy may be due to experimental errors because wire drag is more significant near $r = 0$. Displacement readings are also less reliable there as indicated by the large error bars. However, the divergence of measurements from theory is not as pronounced at the lower level. Since the region near $r = 0$ is of small scale, perhaps this behaviour is another manifestation of the inadequacy of the theory in representing small-scale effects.

Experimental investigation of the stratified spin-up problem has also been conducted by Holton (1965), McDonald & Dicke (1967) and Modisette & Novotny (1969). Holton's experiments demonstrate the essential features of the spin-up flow predicted by theory. His quantitative agreement with theory, however, was fortuitous since his side-wall boundary condition is inappropriate to his experimental condition and the experiments were coarse in nature.

McDonald & Dicke conducted both homogeneous and stratified spin-up experiments and observed the damping of the azimuthal motion of the fluid by the use of free surface floats. The observations were made over a long period (20 min) and at large intervals (one minute) of time. Based on the great difference in the damping rates they were led to conclude that 'the occurrence of Ekman pumping and the ensuing "spin-down" in a fluid can indeed be inhibited or eliminated by a sufficient density gradient in the fluid'. Their stratified experiment is equivalent to our experiment SS 27 ($B = 1{\cdot}44$) at mid-level; the aspect ratios are nearly the same for both experiments. They interpret spin-down of a stratified fluid as an attainment of a state of no motion relative to the container, as is the case in homogeneous fluid spin-down, and have designed their experiment accordingly. We see from the results of experiment SS 27 at mid-level (figure 11) that the effect of the meridional circulation (Ekman pumping) is slight in its penetration and short in duration. The spin-up time, in terms of our definition, is approximately 15 sec. Thus McDonald & Dicke could not easily sense the spin-up process with a surface float on their experimental time resolution and scale. They were observing primarily the viscous diffusion effects, hence their conclusion regarding Ekman pumping in the presence of stratification.

Modisette & Novotny repeated and extended the experiments of McDonald & Dicke. They interpreted McDonald & Dicke's conclusions to mean that convective spin-down can be prevented by a density gradient and they attempted to find a transition between a convective spin-down typical of a homogeneous fluid and a purely viscous 'spin-down'. Experiments were extended by reducing the height of the stratified fluid but maintaining the same density difference across the boundaries. In terms of our parameters, they performed a series of experiments with decreasing values of B/a, with a change in the aspect ratio a by a factor of 10. In effect they observed the mid-level over a range between experiment SS 27, $B/a = 0{\cdot}92$, and experiment SS 24, $B/a = 0{\cdot}31$. They interpreted the decreasing displacement of the surface float with decreasing B/a as evidence of a transition. In actuality, they observed the deeper penetration of the meridional circulation as a result of the decreasing value of B/a rather than a transition between two distinct mechanisms. Their displacement curves at low values of B/a show peculiar curvatures which most probably reflect the coarse nature of their experimental technique.

We have also attempted free-surface experiments similar to those described above. These experiments, however, proved unsuccessful. Experimental measurements obtained with free surface floats and internal markers were in poor and often inconsistent agreement with theory. It was later discovered that the free surface did not behave as a truly free surface in that it acquired rigid surface characteristics. Such characteristics of a free surface are not uncommon and are usually a result of impurities in the fluid at the free surface.

7. Experimental errors

An overall effect of experimental errors such as the uncertainty in time measurement, position of the dye, drag due to wires, and the nature of the turntable response to a change in the rotation rate can be demonstrated by an application of the experimental method to a well-understood flow, namely the spin-up of a homogeneous fluid. A number of homogeneous spin-up experiments were conducted to evaluate and refine the experimental method.

Greenspan & Howard (1963) present a thorough theoretical analysis of the homogeneous spin-up problem as well as experimental results in excellent agreement with their theory. Their results for the azimuthal displacement may be conveniently written in the form

$$\theta - \theta_0 = \Delta\Omega\tau_h(e^{-t/\tau_h} - 1),$$

where θ_0 is the initial position of a fluid element, τ_h is the spin-up time based on the final rotation rate and $\Delta\Omega$ is the change in the rotation rate. The result of a representative experiment conducted with a rigid top surface at a rotation rate of $1{\cdot}1$ rad/sec with a change of rotation rate of $1{\cdot}3$ % and a calculated spin-up time of $61{\cdot}8$ sec is shown in figure 14. Relative displacement is plotted as a function of time in the form e^{-t/τ_h}. In this form, the experimental points should fall on a straight line. Greenspan & Howard's result is given by the solid line and the experimental results obtained at two levels, $z = -0{\cdot}26$ and $z = -0{\cdot}92$, are represented by the dashed line. The error bars over the experimental points indicate the thickness of the dye line at $r = 0{\cdot}5$ and represent approximately the extent of the reading error. The measurements at the two levels agree with each other within experimental error, as they should. The experimental straight line is determined by the experimental data through twice the spin-up time. At larger times, the experimental points fall below the straight line. This departure is due to thermal currents which are driven by small temperature differences between the room and the fluid in the container rather than the spin-up process itself. For small temperature differences these extraneous flows are weak and noticeable only when the flow due to spin-up approaches rigid-body rotation at the new rotation rate. Greenspan & Howard's experiments do not show such an extraneous flow primarily because of the large imposed change in the rotation rate, approximately 15 %, and because of the relatively short time, approximately twice the spin-up time, that the surface float was followed. With such large initial velocity, the velocity after two spin-up times is still large enough so that even a moderate thermal effect may not be noticeable.

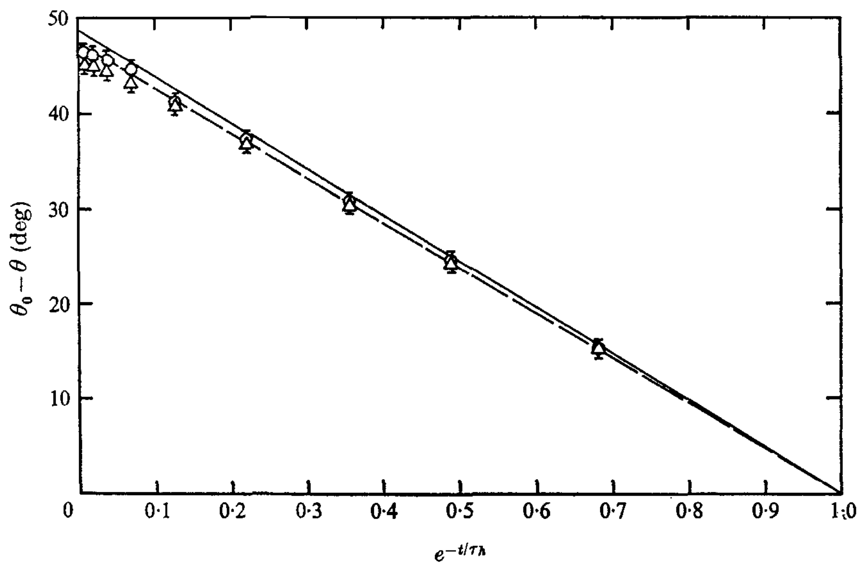

FIGURE 14. The azimuthal displacement field as a function of time for a homogeneous fluid at $\Omega = 1{\cdot}1$ rad/sec and $\Delta\Omega/\Omega = 0{\cdot}013$ with $\tau_h = 61{\cdot}8$ sec. ○, △, experiment at $z = -0{\cdot}92$ and $z = -0{\cdot}26$, respectively; ———, Greenspan & Howard (1963).

The experimental spin-up time calculated from the intercept is 59·9 sec and is approximately 3 % lower than the theoretical prediction. In general, the results obtained from a number of homogeneous spin-up experiments agree with the theoretical calculations with an error of 5 % or less. The experimental spin-up time and displacement, however, generally fall below their theoretical values.

Stratified experiments contain the errors described above as well as additional errors due to the uncertainty in the density gradient, deviations from a linear gradient, and the presence of the Sweet–Eddington flow. The error in the density gradient, based on the different possible slopes through the positions of the floats and the limiting densities, is 2 to 4 %. The corresponding effect on the angular displacement is between 1 and 2 %.

Significant deviations from a linear density gradient occur only near the horizontal boundaries, and are due to molecular diffusion of salt. Although the diffusion process is slow, the 4–5 h from the beginning of the filling process to the time of the experiment are sufficient to create noticeable departure. The dashed curve in figure 5 represents such a deviation after 4 h. The distortion is more representative of the fluid near the top boundary since it is 'older' than the fluid near the bottom boundary. The effect of the distortion of the density gradient on the flow field is difficult to estimate. It is an effect which is not considered in the theory and must be kept in mind in a final evaluation of *quantitative* differences between experiment and theory.

A study of the effect of the above distortion on the flow field was attempted by two experiments described below.

In the first experiment, the top centimetre of fluid normally containing the largest distortion was eliminated by overfilling the container with an appropriate amount of stratified fluid from below. Hence, the density gradient was initially 'linear'. In the second experiment, constant density layers, $\frac{1}{2}$ cm in height, were introduced at the top and bottom boundaries; the top layer consisted of pure water and the bottom layer was at the maximum density of the linear gradient. Both experiments were conducted under conditions similar to experiment SS 14. The results of the two experiments and experiment SS 14 were essentially the same and could not be effectively distinguished. These experiments confirm that there are layers of fluid near the horizontal boundaries where significant departure from a linear density gradient can occur.

Flows extraneous to the spin-up flow occur as a result of thermal effects and the Sweet–Eddington flow. Thermal effects of the type noted in the homogeneous spin-up experiments do not occur here because large-scale motions due to small temperature variations in the fluid are inhibited by the relatively large density gradient. However, motion in small-scale cells is still possible. Superimposed on the possible weak thermal flow is the Sweet–Eddington flow. The combined effect of these two flows is small for experiments conducted at rotation rates of 1 rad/sec or less. The resulting angular displacement over the duration of the spin-up process is usually less than two degrees, or typically less than 2 % of the total angular displacement.

Errors arising from the approximation inherent in the theory are generally less than or of the order of the various errors considered above. For most experiments the variation of density between the top or bottom boundary and the mid-level is from 2 to 6 %, and the terms neglected in the Boussinesq approximation are at most 2 to 6 % of those retained, depending on the extent of the stratification. The kinematic viscosity of the fluid also varies from 2 to 6 % between the mid-level and a horizontal boundary. Thus the kinematic viscosity may be considered constant within the Boussinesq approximation.

We are grateful to the National Science Foundation which supported this research through Grants GA-872, GA-1416 and GA-11410. One of us (G.B.) completed the writing of the text with support from ONR contract N00014-68-A-0159.

REFERENCES

Baker, D. J. 1966 *J. Fluid Mech.* **26**, 573.

Ekman, V. W. 1906 *Ann. d. Hydr.* **34**, 23.

Fortuin, J. M. H. 1960 *J. Polymer Sci.* **44**, 505.

Greenspan, H. P. 1968 *The Theory of Rotating Fluids.* Cambridge University Press.

Greenspan, H. P. & Howard, L. N. 1963 *J. Fluid Mech.* **17**, 385.

Holton, J. R. 1965 *J. Atmos. Sci.* **22**, 402.

McDonald, B. E. & Dicke, R. H. 1967 *Science*, **158**, 1562.

Modisette, J. L. & Novotny, J. E. 1969 *Science*, **166**, 872.

Pedlosky, J. 1967 *J. Fluid Mech.* **28**, 463.

Pettersson, H. 1931 *Göteborgs Kungl. Vetenskaps och Vitterhets-Samhälles Handlingar*, **2**, 3.

Sakurai, T. 1969 *J. Fluid Mech.* **37**, 689.

Walin, G. 1969 *J. Fluid Mech.* **36**, 289.

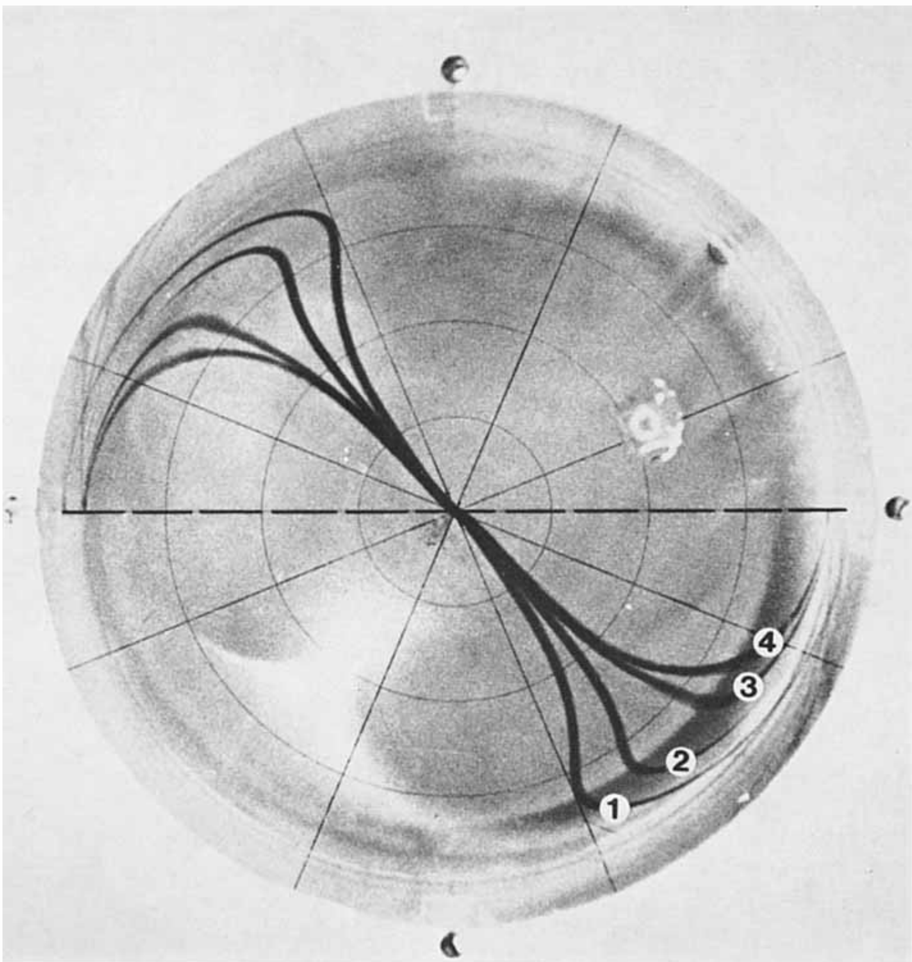

FIGURE 9. A photograph of the azimuthal displacement field as a function of radius and height after 61 sec for $B = 0{\cdot}684$ and $\Delta\Omega/\Omega = 0{\cdot}021$ (experiment SS31) at the levels: (1) $z = -0{\cdot}005$, (2) $z = -0{\cdot}58$, (3) $z = -0{\cdot}83$, and (4) $z = -0{\cdot}92$. Fluid motion is clockwise relative to the container. The initial position of the dye lines is represented by the dashed line drawn on the photograph.

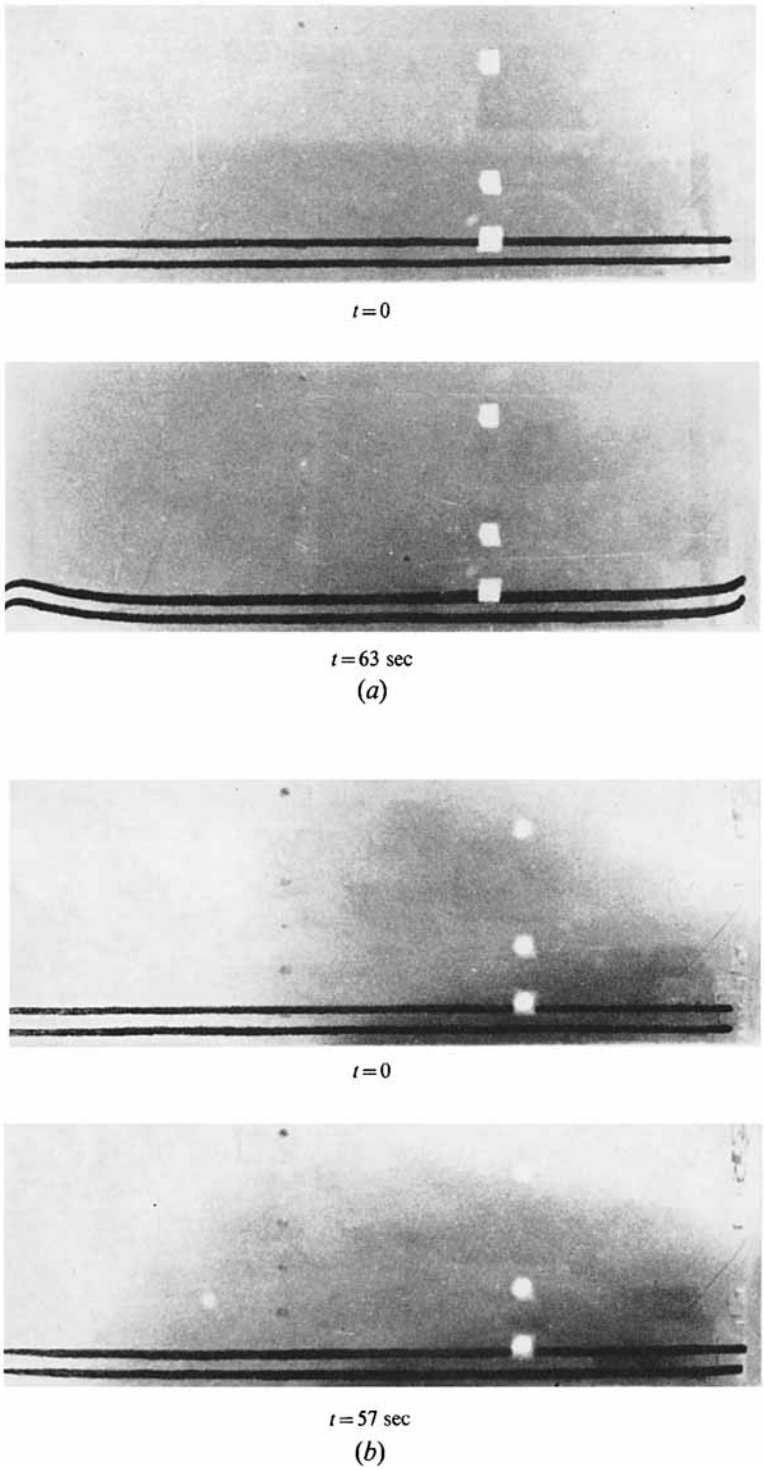

FIGURE 12. Photographs of the meridional circulation as viewed from the side of the container. (*a*) Homogeneous spin-up, $\Omega = 1{\cdot}11$ rad/sec, $\Delta\Omega/\Omega = 0{\cdot}019$, $\tau_h = 62$ sec. (*b*) Stratified spin-up, $B = 0{\cdot}79$, $\Omega = 1{\cdot}10$ rad/sec, $\Delta\Omega/\Omega = 0{\cdot}015$ at the levels $z = -0{\cdot}83$ and $-0{\cdot}92$, $\tau/\tau_h = 0{\cdot}59$ at $z = -0{\cdot}83$ and $r/a = 0{\cdot}5$. The dye lines in the photographs were touched up to make the dye appear darker.

BUZYNA AND VERONIS

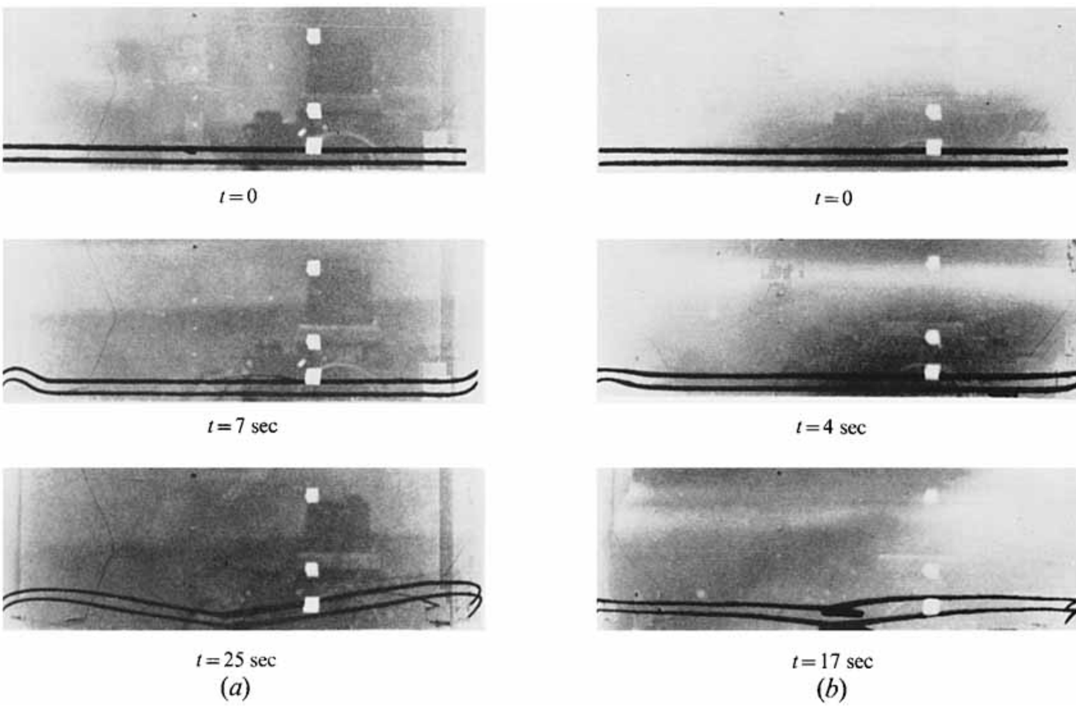

FIGURE 13. Photographs of the meridional circulation as viewed from the side of the container. (*a*) Homogeneous spin-up, $\Omega = 1{\cdot}17$ rad/sec, $\Delta\Omega/\Omega = 0{\cdot}073$, $\tau_h = 60$ sec. (*b*) Stratified spin-up, $B = 0{\cdot}70$, $\Omega = 1{\cdot}24$ rad/sec, $\Delta\Omega/\Omega = 0{\cdot}11$ at the levels $z = -0{\cdot}83$ and $z = -0{\cdot}92$, $\tau/\tau_h = 0{\cdot}65$ at $z = -0{\cdot}83$ and $r/a = 0{\cdot}5$. The dye lines in the photographs were touched up to make the dye appear darker.